

# BIOREMEDIATION SCIENCE AND TECHNOLOGY RESEARCH

Website: <http://journal.hibiscuspublisher.com/index.php/BSTR/index>



## Mathematical Modeling of Molybdenum Blue Production from *Serratia marcescens* strain DR.Y10

Othman, A.R.<sup>1</sup>, Johari, W.L.W.<sup>2</sup>, Dahalan, F.A.<sup>3</sup> and Shukor, M.Y.\*<sup>1</sup>

<sup>1</sup>Department of Biochemistry, Faculty of Biotechnology and Biomolecular Sciences, Universiti Putra Malaysia, UPM 43400 Serdang, Selangor, Malaysia.

<sup>2</sup>Department of Environment, Faculty of Environmental Studies, Universiti Putra Malaysia, 43400 UPM Serdang, Selangor, Malaysia.

<sup>3</sup>School of Environmental Engineering, Kompleks Pusat Pengajian Jejawi 3, Universiti Malaysia Perlis, 02600 Arau, Perlis, Malaysia.

\*Corresponding author:

Assoc. Prof. Dr. Mohd Yunus Shukor,  
 Department of Biochemistry,  
 Faculty of Biotechnology and Biomolecular Sciences,  
 Universiti Putra Malaysia,  
 UPM 43400 Serdang,  
 Selangor, Malaysia.

Email: [mohdyunus@upm.edu.my/yunus.upm@gmail.com](mailto:mohdyunus@upm.edu.my/yunus.upm@gmail.com)

### HISTORY

Received: 16<sup>th</sup> September 2015  
 Received in revised form: 29<sup>th</sup> November 2015  
 Accepted: 20<sup>th</sup> of December 2015

### KEYWORDS

molybdenum reduction  
 metal detoxification  
 molybdenum blue  
*Serratia marcescens*  
 modified Gompertz

### ABSTRACT

The pollution of heavy metals and toxic xenobiotics has become a central issue worldwide. Bioremediation of these toxicants are being constantly carried out using novel microbes. Molybdenum reduction to molybdenum blue is a detoxification process and mathematical modelling of the reduction process can reveal important parameters such as specific reduction rate, theoretical maximum reduction and whether reduction at high molybdenum concentration affected the lag period of reduction. The used of linearization method through the use of natural logarithm transformation, although popular, is inaccurate and can only give an approximate value for the sole parameter measured; the specific growth rate. In this work, a variety of models for such as logistic, Gompertz, Richards, Schnute, Baranyi-Roberts, Von Bertalanffy, Buchanan three-phase and more recently Huang were utilized for the first time to obtain values for the above parameters or constants. The modified Gompertz model was the best model in modelling the Mo-blue production curve from *Serratia marcescens* strain DR.Y10 based on statistical tests such as root-mean-square error (RMSE), adjusted coefficient of determination ( $R^2$ ), bias factor (BF), accuracy factor (AF) and corrected AICc (Akaike Information Criterion). Parameters obtained from the fitting exercise were maximum Mo-blue production rate ( $\mu_m$ ), lag time ( $\lambda$ ) and maximal Mo-blue production ( $Y_{max}$ ) of X ( $h^{-1}$ ), Y (h) and Z (nmole Mo-blue), respectively. The application of primary population growth models in modelling the Mo-blue production rate from this bacterium has become a successful undertaking. The model may also be used in other heavy metals detoxification processes. The parameters constants extracted from this work will be a substantial help for the future development of further secondary models.

### INTRODUCTION

Bacterial growth linked processes frequently display a unique phase in which the specific growth rate commences at a value of zero after which it accelerates to a maximal value ( $\mu_{max}$ ) in a

certain time period, producing a lag time ( $\lambda$ ). It has been argued that the lag period seen in the sigmoid shape is because the bacterial cells are gearing their growth mechanism to adjust to a new environment having been in a vegetative state especially during storage. This adjustment period is traditionally called the

lag period. It has been suggested as a transient period that connects two autonomous systems. The introduction of the lag time or parameter is meant largely convenience rather than having a mechanistic interpretation [1]. It is theorized that in the initial inocula, each bacterial cells would have different rates of growth and if these rates, if they could be measured, would show nonlinear distribution as suggested by several workers [1,2].

Molybdenum has many uses in industries including alloying agent, automobile engine anti-freeze component, portion of corrosion resistant steel and as lubricant in the form of molybdenum disulphide. The wide application of molybdenum in industry has triggered several water pollution cases worldwide such as in the Tokyo Bay, Tyrol in Austria and in the Black Sea, where molybdenum level reaches in the hundreds of ppm [3]. In addition, terrestrially, it has been recognized as a significant pollutant in sewage sludge pollution that poses a health hazard [3].

Molybdenum is very toxic to ruminants at levels of several parts per million, with cows being the most affected [4,5]. As to date quite a number of Mo-reducing bacterium has been isolated, and most of these bacterium were isolated locally [6–13,13,14] with the exception of a few [15–18]. The perceived low toxicity of molybdenum to human and other organism compared to other heavy metals such as mercury, selenium and chromium has resulted in not many works on molybdenum reduction as a detoxification process. However, more recent data on molybdenum toxicity in inhibiting spermatogenesis and arresting embryogenesis in organisms such as catfish and mice at levels as low as several parts per million [19,20] will spur more works on microbial molybdenum detoxification in the near future.

Kinetic studies on Mo-blue production have been explored previously [8,21] but all of these works utilize the linearization of the Mo-blue production over time profile to obtain the specific growth rate for further secondary modelling. As the benefits of nonlinear regression analysis of the Mo-blue production have been described above, thus, the objective of this work is to evaluate several available models such as Logistic [22,23], Gompertz [23,24], Richards [23,25], Schnute [23], Baranyi-Roberts [26], Von Bertalanffy [27,28], Buchanan three-phase [29] and more recently Huang model [30] in modeling Mo-blue production from the bacterium *Serratia marcescens* strain DR.Y10.

## MATERIALS AND METHODS

### Isolation and maintenance of the Molybdate-reducing bacterium

The bacterium utilized in this work has been previously developed as an assay for the heavy metal lead [31]. The growth and maintenance was carried out on solid agar in low phosphate media (pH 7.0) containing glucose (1%),  $(\text{NH}_4)_2\text{SO}_4$  (0.3%),  $\text{MgSO}_4 \cdot 7\text{H}_2\text{O}$  (0.05%), NaCl (0.5%), yeast extract (0.05%),  $\text{Na}_2\text{MoO}_4 \cdot 2\text{H}_2\text{O}$  (0.242%) and  $\text{Na}_2\text{HPO}_4$  (0.071% or 5 mM) (Abo-Shakeer et al., 2013). Glucose was separately autoclaved.

### Preparation of resting cells for molybdenum reduction characterization

Monitoring of Mo-blue production at various sodium molybdate concentration was carried out statically using resting cells in a microplate or microtiter format as previously developed [32]. Cells from a 1 L overnight culture grown in High Phosphate media (HPM) at room temperature on orbital shaker (150 rpm)

with the only difference between the LPM and HPM was the phosphate concentration which was fixed at 100 mM for the HPM. Cells harvesting was carried out by centrifugation at  $15,000 \times g$  for 10 minutes. The pellet was washed several times to remove residual phosphate and resuspended in 20 mls of low phosphate media (LPM) minus molybdenum to an absorbance at 600 nm of approximately 1.00. Higher concentrations were found to be strongly inhibitory to molybdate reduction [6–8,10,33–37]. Then 180  $\mu\text{L}$  was sterically pipetted into each well of a sterile microplate. Various sodium molybdate concentrations in a volume of 20  $\mu\text{L}$  from a stock solution was then added to each well to initiate Mo-blue production. A sterile sealing tape that allows gas exchange (Corning® microplate) was used for sealing the tape. The microplate was incubated at room temperature. At defined times absorbance at 750 nm was read in a BioRad (Richmond, CA) Microtiter Plate reader (Model No. 680). The production of Mo-blue from the media in a microplate format was measured using the specific extinction coefficient of  $11.69 \text{ mM}^{-1} \cdot \text{cm}^{-1}$  at 750 nm as the maximum filter wavelength available for the microplate unit was 750 nm [38].

### Determination of Kinetic Parameters for Molybdenum Blue production

#### Fitting of the data

Fitting of the growth data to the nonlinear equations (Table 1) were carried out by nonlinear regression utilizing the Marquardt algorithm that minimizes sums of square of residuals utilizing CurveExpert Professional software (Version 1.6). In this lookup approach, the sum of the squares of the differences between the predicted and observed values is minimized. The software can be automatically or manually programmed to calculate initial values of parameters. Estimation of  $\mu_m$  was carried out by the steepest ascent search of the curve amongst four datum points. Estimation of  $\lambda$  was carried out by determining the intersection of this line with the x axis. Finally, estimation for the asymptote (A) was carried out by taking the final datum point. As the Huang's model is a differential equation, it needs to be solved numerically. The Runge-Kutta method was utilized to solve numerically the differential equation. The ode45 solver in MATLAB (Version 7.10.0499, The MathWorks, Inc., Natick, MA) was used to solve this equation.

#### Statistical analysis

To make a decision whether there's a statistically significant difference between models with different number of parameters, with regards to the quality of fit to the same experimental data was statistically evaluated through numerous methods including the corrected AICc (Akaike Information Criterion), Root-Mean-Square Error (RMSE), bias factor (BF), accuracy factor (AF), and adjusted coefficient of determination ( $R^2$ ).

The RMSE was calculated according to Eq. (1), where  $Ob_i$  is the experimental data,  $Pd_i$  are the values predicted by the model,  $n$  is the number of experimental data and  $p$  is the number of parameters of the assessed model. It is anticipated that the model with the smaller number of parameters will give a smaller RMSE values [39].

$$RMSE = \sqrt{\frac{\sum_{i=1}^n (Pd_i - Ob_i)^2}{n - p}} \quad (1)$$

The coefficient of determination or  $R^2$  is used to assess the quality of fit of a model in linear regression. However, in

nonlinear regression where difference in the number of parameters between one models to another do vary, the adoption of the  $R^2$  method does not readily provides comparable analysis. In order to solve this issue, the adjusted  $R^2$  is used to calculate the quality of nonlinear models using equations 2 and 3 according to the formula where  $s_y^2$  is the total variance of the y-variable and RMS is Residual Mean Square.

$$\text{Adjusted } (R^2) = 1 - \frac{\text{RMS}}{s_y^2} \quad (2)$$

$$\text{Adjusted } (R^2) = 1 - \frac{(1 - R^2)(n-1)}{(n-p-1)} \quad (3)$$

The Akaike Information Criterion (AIC) supplies a solution to model selection by way of computing the relative quality of a given statistical model for just about any given set of experimental data [40]. AIC handles the trade-off in regards to the goodness of fit of the model as well as the complexness of the model. It is in reality founded on information theory. The method offers a comparative approximation of the information lost for each and every time a given model is used to represent the process that produces the information or data. For an output of a set of predicted model, the most accepted model will be the model displaying the minimum value for AIC. This value is generally a negative value, with by way of example; an AICc value of -10 is more recommended than the one with -1. The equation includes number of parameters penalty, the more the number of parameters, the less desired the output or the higher the AIC value. Hence, AIC not simply rewards goodness of fit, but additionally does not encourage utilizing more complex model (overfitting) for fitting experimental data. For data having a smaller number of values or a high number of parameter used, a corrected version of AIC, the Akaike information criterion (AIC) with correction or AICc is utilized instead [41]. The AICc is calculated for each data set for each model according to the following equation (Eqn. 4);

$$\text{AICc} = 2p + n \ln \left( \frac{\text{RSS}}{n} \right) + 2(p+1) \frac{2(p+1)(p+2)}{n-p-2} \quad (4)$$

Where  $n$  represent the number of data points in the curve and  $p$  represents the number of parameters used in the model. The procedure considers the alteration in goodness-of-fit and the difference in number of parameters between two models. For each data set, the model having the smallest AICc value is more likely correct [41].

Accuracy Factor (AF) and Bias Factor (BF) to test for the goodness-of-fit of the models was calculated according to Eqns. 5 and 6 as suggested and first proposed by Ross [42]. A Bias Factor that is equal to 1 signifies an ideal match between observed and predicted values. For microbial growth curves or Mo-blue production studies, a bias factor having values < 1 signifies a fail-dangerous model whilst a bias factor having values > 1 signifies a model that is fail-safe. The value of the Accuracy Factor is usually  $\geq 1$ , with higher AF values signifies prediction that is less precise or accurate.

$$\text{Bias factor} = 10^{\left( \sum_{i=1}^n \log \left( \frac{Pd_i / Ob_i}{n} \right) \right)} \quad (5)$$

$$\text{Accuracy factor} = 10^{\left( \sum_{i=1}^n \log \left( \frac{Pd_i / Ob_i}{n} \right) \right)} \quad (6)$$

**Table 1.** Mo-blue production models used in this study.

No Model	No of parameters	Equation
1 Modified Logistic	3	$y = \frac{A}{\left\{ 1 + \exp \left[ \frac{4 \mu_m}{A} (\lambda - t) + 2 \right] \right\}}$
2 Modified Gompertz	3	$y = A \exp \left\{ - \exp \left[ \frac{\mu_m e}{A} (\lambda - t) + 1 \right] \right\}$
3 Modified Richards	4	$y = A \left\{ 1 + v \exp(1+v) \exp \left[ \frac{\mu_m}{A} (1+v) \left( 1 + \frac{1}{v} \right) (\lambda - t) \right] \right\}^{\left( \frac{-1}{v} \right)}$
4 Modified Schnute	4	$y = \left( \mu_m \frac{(1-\beta)}{\alpha} \right) \left[ \frac{1 - \beta \exp(\alpha \lambda + 1 - \beta - \alpha t)}{1 - \beta} \right]^{\frac{1}{\beta}}$
5 Baranyi-Roberts	4	$y = A + \mu_m x + \frac{1}{\mu_m} \ln \left( e^{-\mu_m x} + e^{-h_0} - e^{-\mu_m x - h_0} \right)$ $- \ln \left( 1 + \frac{\mu_m x + \frac{1}{\mu_m} \ln \left( e^{-\mu_m x} + e^{-h_0} - e^{-\mu_m x - h_0} \right)}{e^{(y_{\max} - A)}} \right)^{-1}$
6 Von Bertalanffy	3	$y = K \left[ 1 - \left[ 1 - \left( \frac{A}{K} \right)^3 \right] \exp \left( - \left( \mu_m x / 3 K \right)^{\frac{1}{3}} \right) \right]^3$
7 Huang	4	$y = A + y_{\max} - \ln \left( e^A + \left( e^{y_{\max}} - e^A \right) e^{-\mu_m B(x)} \right)$ $B(x) = x + \frac{1}{\alpha} \ln \frac{1 + e^{-\alpha(x-\lambda)}}{1 + e^{\alpha \lambda}}$
8 Buchanan Three-phase linear model	3	$Y = A, \text{ IF } X < \text{LAG}$ $Y = A + K(X - \lambda), \text{ IF } \lambda \leq X \leq X_{\max}$ $Y = Y_{\max}, \text{ IF } X \geq X_{\max}$

Note:

A= Mo-blue lower asymptote;

$\mu_m$ = maximum specific Mo-blue production rate;

v= affects near which asymptote maximum Mo-blue production occurs.

$\lambda$ =lag time

$y_{\max}$ = Mo-blue upper asymptote;

e = exponent (2.718281828)

t = sampling time

$\alpha, \beta, k$  = curve fitting parameters

$h_0$  = a dimensionless parameter quantifying the initial physiological state of the reduction process. The lag time ( $h^{-1}$ ) can be calculated as

$h_0 = \mu_{\max}$

## RESULTS AND DISCUSSION

The Mo-blue production from this bacterium was sigmoidal in shape with a lag phase of about 15 hours and reaching maximum Mo-blue production at approximately 50 hours of static incubation (**Fig. 1**). The Mo-blue production over time profile was fitted to eight different models. The resultant fitting shows visually acceptable fitting (**Fig. 2**). The best performance was modified Gompertz model with the lowest value for RMSE, AICc and the highest value for adjusted  $R^2$ . The AF and BF values were also excellent for the model with their values were the closest to 1.0. The poorest performance was Von Bertalanffy with the lowest score for most of the statistics tests

(Table 2). The coefficients for the modified Gompertz model at various molybdenum concentrations are shown in Table 3.

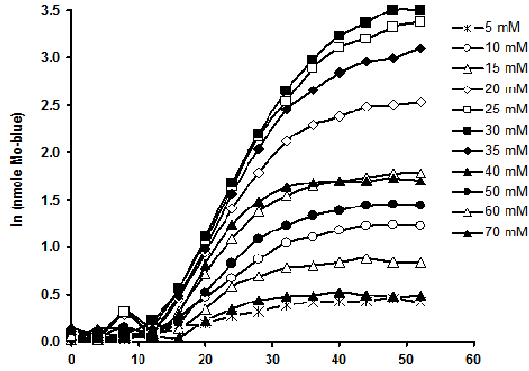


Fig. 1. The Mo-blue production curves of *Serratia marcescens* strain DR.Y10 at various concentrations of sodium molybdate over time. The error bars represent mean  $\pm$  standard deviation of three replicates.

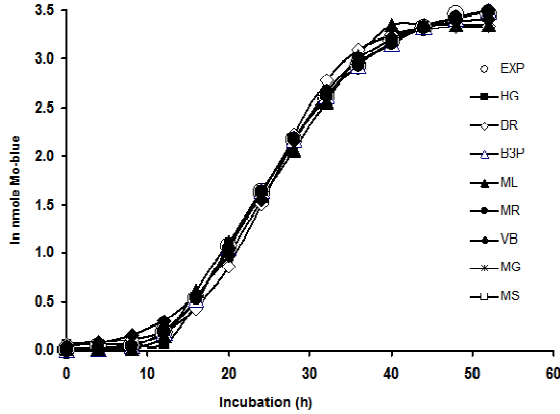


Fig. 2. The Mo-blue production curve of *Serratia marcescens* strain DR.Y10 at 30 mM of sodium molybdate fitted to various models. The models utilized were Huang (HG), Baranyi-Roberts (BR), Buchanan-three phase (B3P), modified Logistics (ML), modified Richards (MR), von Bertalanffy (VB), modified Gompertz (MG) and modified Schnute (MS).

Table 2 Statistical analysis of the various fitted models.

Model	Parameter	RMSE	R <sup>2</sup>	adR <sup>2</sup>	AICc	BF	AF
Huang	4	0.048	0.999	0.999	64.15	1.11	1.24
Baranyi-Roberts	4	0.128	0.994	0.991	86.06	1.20	1.27
Buchanan-3-phase	3	0.020	0.994	0.993	-94.76	1.01	1.09
modified Logistics	3	0.089	0.997	0.996	-52.55	0.99	1.20
modified Richards	4	0.022	0.992	0.990	-86.42	0.82	1.24
von Bertalanffy	3	0.101	0.996	0.994	-49.04	0.58	1.88
modified Gompertz	3	0.022	0.997	0.999	-99.99	0.99	1.26
modified Schnute	4	0.089	0.997	0.999	-27.00	1.24	1.26

Note:  
 $p$  no of parameters  
 $adR^2$  Adjusted Coefficient of determination  
 $BF$  Bias factor  
 $AF$  Accuracy factor

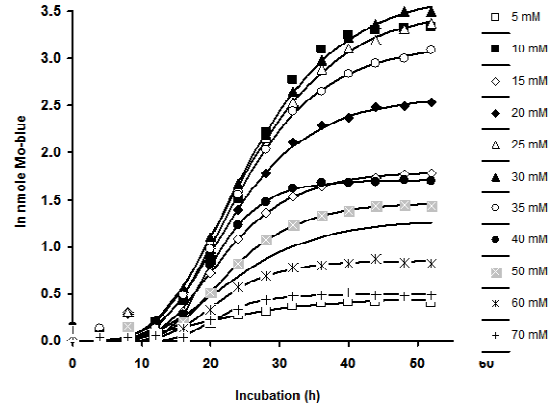


Fig. 3. The Mo-blue production curves of *Serratia marcescens* strain DR.Y10 on various concentrations of sodium molybdate fitted using the Gompertz model.

Table 3. Mo-blue production coefficients at various molybdenum concentrations as modelled using the modified Gompertz model.

	Molybdenum concentration											
	5 mM	10 mM	15 mM	20 mM	25 mM	30 mM	35 mM	40 mM	50 mM	60 mM	70 mM	
Asymptote (ln nmole Mo-blue)	0.45	1.29	1.80	2.59	3.54	3.69	3.14	1.71	1.47	0.86	0.50	
$\mu_m$ (h <sup>-1</sup> )	0.02	0.06	0.10	0.12	0.14	0.15	0.14	0.13	0.08	0.06	0.04	
lag (h)	6.92	11.37	12.36	12.13	12.07	12.45	12.89	13.86	13.56	13.44	15.07	

The modified Gompertz model is one of the classical growth models that include model such as the Verhulst [23,24]. The Gompertz function, named in 1844-1845 by Pierre Franois Verhulstis, is based on an exponential relationship between specific growth rate and population density (Eqn x). The initial stage of growth is approximately exponential; then, as saturation begins, the growth slows, and at maturity, growth stops. Gibson et al. [43] were the first to use the Gompertz equation to fit microbial growth curves and the equation was successfully used to describe the exponential and stationary phases of the microbial growth curves that is sigmoidal. However, the model was not adequate to describe the lag phase. The model was modified by Gibson et al. [43] to incorporate the lag phase, and have been successfully used in modelling many microbial growth curves to the point where its dominance in mathematically modelling bacterial growth and product formation curves have been acknowledged [23,28,44]. The model is expressed as follows (Eqn 7):

$$N = D \exp \left( - \exp \left( \frac{B}{M} (t - M) \right) \right) \quad (7)$$

$N$  = the difference in product concentration, optical density or log cfu/ml value of the upper and lower asymptotes  
 $M$  = the maximum product concentration, death or growth rates at time  $M$  (h<sup>-1</sup>)  
 $t$  = the time at which the absolute production, death or growth rates at maximum occur (h)  
 $A_g$  = the lower asymptote value of the product concentration, optical density or log cfu/ml

The model has its drawbacks and is not perfect with several main issues. Firstly, in the static version,  $N_{(t=0)}$  is not equal to  $N_0$ . Secondly, an inflection point is the intrinsic property of the sigmoidal curve causing the model to have a systematic problem in describing the exponential phase (Baranyi et al., 1993). Finally, the model tend to over-estimates its parameter values [45–47].

The asymmetrical sigmoidal shape of the modified Gompertz represents and may offer greater flexibility than the logistic. Sigmoidal models such as the logistic and Gompertz differ chiefly at the point of inflection between the lower and the upper asymptotes with the logistics and Gompertz models having the distance of 1/2 and 1/e between the lower and the upper asymptotes, respectively [28]. In an essence, other growth models provide flexible slope function and variable point of inflection between the lower and upper asymptotes. These functions are either special or simpler cases of a parent growth model. For instance, the Richard model incorporates the logistics, Gompertz or von Bertalanffy growth models [23,28,43].

Parameters obtained from the fitting exercise would be later used for secondary modelling of Mo-blue production using model such as the two-parameter Monod model or other more complex models "secondary models" such as Haldane, Aiba, Yano and others. These mechanistic models are used in basic research and are aimed to reach a better understanding of the physical, chemical and biological processes that lead to the growth profile seen. All other things being equal, mechanistic models are more powerful since they tell you about the underlying processes driving patterns. They are more likely to work correctly when extrapolating beyond the observed conditions [48].

## CONCLUSION

In conclusion, the Gompertz model was the best model in modelling the Mo-blue production curve of the bacterium *Serratia marcescens* strain DR.Y10 based on statistical tests such as root-mean-square error (RMSE), adjusted coefficient of determination ( $R^2$ ), bias factor (BF), accuracy factor (AF) and corrected AICc (Akaike Information Criterion). Parameters obtained from the fitting exercise were maximum Mo-blue production rate ( $\mu_m$ ), lag time ( $\lambda$ ) and maximal Mo-blue production ( $Y_{max}$ ) of X ( $h^{-1}$ ), Y (h) and Z (nmole Mo-blue), respectively. The use of bacterial growth models to obtained accurate Mo-blue production rate useful for further secondary model development is novel for molybdenum reduction to Mo-blue specifically and in heavy metals detoxification process in general as judged from literature search, and this work has demonstrated the applicability of such models. Current works include secondary modelling of the Mo-blue production from this bacterium especially on the inhibitory effect of the substrate molybdenum on the maximum Mo-blue production rate values obtained from this works. In addition, other secondary modelling works including the effect of environmental conditions (pH and temperature) on Mo-blue production rates are being carried out.

## ACKNOWLEDGEMENT

This work was supported by the research grant from the Ministry of Science, Technology and Innovation [MOSTI] under Science Fund grant no: 02-03-08-SF0061.

## REFERENCES

1. Baranyi J, Roberts TA. A dynamic approach to predicting bacterial growth in food. *Int J Food Microbiol*. 1994;23(3-4):277-94.
2. Buchanan RL, Whiting RC, Damert WC. When is simple good enough: A comparison of the Gompertz, Baranyi, and three-phase

- linear models for fitting bacterial growth curves. *Food Microbiol*. 1997;14(4):313-26.
3. Neunhäuserer C, Berreck M, Insam H. Remediation of soils contaminated with molybdenum using soil amendments and phytoremediation. *Water Air Soil Pollut*. 2001;128(1-2):85-96.
4. Underwood EJ. Environmental sources of heavy metals and their toxicity to man and animals. 1979;11(4-5):33-45.
5. Kincaid RL. Toxicity of ammonium molybdate added to drinking water of calves. *J Dairy Sci*. 1980;63(4):608-10.
6. Abo-Shakeer LKA, Ahmad SA, Shukor MY, Shamaan NA, Syed MA. Isolation and characterization of a molybdenum-reducing *Bacillus pumilus* strain lbna. *J Environ Microbiol Toxicol*. 2013;1(1):9-14.
7. Lim HK, Syed MA, Shukor MY. Reduction of molybdate to molybdenum blue by *Klebsiella* sp. strain hkeem. *J Basic Microbiol*. 2012;52(3):296-305.
8. Othman AR, Bakar NA, Halmi MIE, Johari WLW, Ahmad SA, Jirangon H, et al. Kinetics of molybdenum reduction to molybdenum blue by *Bacillus* sp. strain A.rzi. *BioMed Res Int*. 2013;2013:Article number 371058.
9. Shukor MY, Ahmad SA, Nadzir MMM, Abdullah MP, Shamaan NA, Syed MA. Molybdate reduction by *Pseudomonas* sp. strain DRY2. *J Appl Microbiol*. 2010;108(6):2050-8.
10. Shukor MY, Habib SHM, Rahman MFA, Jirangon H, Abdullah MPA, Shamaan NA, et al. Hexavalent molybdenum reduction to molybdenum blue by *S. marcescens* strain Dr. Y6. *Appl Biochem Biotechnol*. 2008;149(1):33-43.
11. Shukor MY, Rahman MF, Shamaan NA, Syed MS. Reduction of molybdate to molybdenum blue by *Enterobacter* sp. strain Dr.Y13. *J Basic Microbiol*. 2009;49(SUPPL. 1):S43-54.
12. Shukor MY, Rahman MF, Suhaili Z, Shamaan NA, Syed MA. Hexavalent molybdenum reduction to Mo-blue by *Acinetobacter calcoaceticus*. *Folia Microbiol (Praha)*. 2010;55(2):137-43.
13. Shukor MY, Rahman MF, Suhaili Z, Shamaan NA, Syed MA. Bacterial reduction of hexavalent molybdenum to molybdenum blue. *World J Microbiol Biotechnol*. 2009;25(7):1225-34.
14. Yunus SM, Hamim HM, Anas OM, Aripin SN, Arif SM. Mo (VI) reduction to molybdenum blue by *Serratia marcescens* strain Dr. Y9. *Pol J Microbiol*. 2009;58(2):141-7.
15. Campbell AM, Del Campillo-Campbell A, Villaret DB. Molybdate reduction by *Escherichia coli* K-12 and its chl mutants. *Proc Natl Acad Sci U S A*. 1985;82(1):227-31.
16. Capaldi A, Proskauer B. Beiträge zur Kenntniss der Säurebildung bei Typhus-bacillen und Bacterium coli - Eine differential-diagnostische Studie. *Z Für Hyg Infect*. 1896;23(3):452-74.
17. Khan A, Halmi MIE, Shukor MY. Isolation of Mo-reducing bacterium in soils from Pakistan. *J Environ Microbiol Toxicol*. 2014;2(1):38-41.
18. Levine VE. The reducing properties of microorganisms with special reference to selenium compounds. *J Bacteriol*. 1925;10(3):217-63.
19. Yamaguchi S, Miura C, Ito A, Agusa T, Iwata H, Tanabe S, et al. Effects of lead, molybdenum, rubidium, arsenic and organochlorines on spermatogenesis in fish: Monitoring at Mekong Delta area and in vitro experiment. *Aquat Toxicol*. 2007;83(1):43-51.
20. Zhang Y-L, Liu F-J, Chen X-L, Zhang Z-Q, Shu R-Z, Yu X-L, et al. Dual effects of molybdenum on mouse oocyte quality and ovarian oxidative stress. *Syst Biol Reprod Med*. 2013;59(6):312-8.
21. Halmi MIE, Ahmad SA, Syed MA, Shamaan NA, Shukor MY. Mathematical modelling of the molybdenum reduction kinetics in *Bacillus pumilus* strain lbna. *Bull Environ Sci Manag*. 2014;2(1):24-9.
22. Ricker, F.J. 11 Growth Rates and Models. In: W.S. Hoar DJR and JRB, editor. *Fish Physiology* [Internet]. Academic Press; 1979 [cited 2014 Jun 27]. p. 677-743. (Bioenergetics and Growth; vol. Volume 8). Available from: <http://www.sciencedirect.com/science/article/pii/S1546509808600345>
23. Zwietering MH, Jongenburger I, Rombouts FM, Van't Riet K. Modeling of the bacterial growth curve. *Appl Environ Microbiol*. 1990;56(6):1875-81.
24. Gompertz B. On the nature of the function expressive of the law of human mortality, and on a new mode of determining the value

- of life contingencies. *Philos Trans R Soc London*. 1825;115:513–85.
25. Richards, F.J. A flexible growth function for empirical use. *J Exp Bot*. 1959;10:290–300.
  26. Baranyi J. Mathematics of predictive food microbiology. *Int J Food Microbiol*. 1995;26(2):199–218.
  27. Babák L, Šupinová P, Burdychová R. Growth models of *Thermus aquaticus* and *Thermus scotoductus*. *Acta Univ Agric Silv Mendel Brun*. 2012;60(5):19–26.
  28. López S, Prieto M, Dijkstra J, Dhanoa MS, France J. Statistical evaluation of mathematical models for microbial growth. *Int J Food Microbiol*. 2004;96(3):289–300.
  29. Buchanan RL. Predictive food microbiology. *Trends Food Sci Technol*. 1993;4(1):6–11.
  30. Huang L. Optimization of a new mathematical model for bacterial growth. *Food Control*. 2013;32(1):283–8.
  31. Ahmad SA, Halmi MIE, Wasoh MH, Johari WLW, Shukor MY, Syed, M.A. The development of a specific inhibitive enzyme assay for the heavy metal, lead. *J Environ Bioremediation Toxicol*. 2013;1(1):9–13.
  32. Shukor MS, Shukor MY. A microplate format for characterizing the growth of molybdenum-reducing bacteria. *J Environ Microbiol Toxicol*. 2014;2(2):42–4.
  33. Ghani B, Takai M, Hisham NZ, Kishimoto N, Ismail AKM, Tano T, et al. Isolation and characterization of a Mo6+-reducing bacterium. 1993;59(4):1176–80.
  34. Shukor Y, Adam H, Ithnin K, Yunus I, Shamaan NA, Syed A. Molybdate reduction to molybdenum blue in microbe proceeds via a phosphomolybdate intermediate. *J Biol Sci*. 2007;7(8):1448–52.
  35. Rahman MFA, Shukor MY, Suhaili Z, Mustafa S, Shamaan NA, Syed MA. Reduction of Mo(VI) by the bacterium *Serratia* sp. strain DRY5. *J Environ Biol*. 2009;30(1):65–72.
  36. Ahmad SA, Shukor MY, Shamaan NA, Mac Cormack WP, Syed MA. Molybdate reduction to molybdenum blue by an antarctic bacterium. *BioMed Res Int*. 2013;2013.
  37. Halmi MIE, Zuhainis SW, Yusof MT, Shaharuddin NA, Helmi W, Shukor Y, et al. Hexavalent molybdenum reduction to Mo-blue by a Sodium-Dodecyl-Sulfate-degrading *Klebsiella oxytoca* strain DRY14. *BioMed Res Int*. 2013;2013:e384541.
  38. Shukor MY, Lee CH, Omar I, Karim MIA, Syed MA, Shamaan NA. Isolation and characterization of a molybdenum-reducing enzyme in *Enterobacter cloacae* strain 48. *Pertanika J Sci Technol*. 2003;11(2):261–72.
  39. Motulsky HJ, Ransnas LA. Fitting curves to data using nonlinear regression: a practical and nonmathematical review. *FASEB J Off Publ Fed Am Soc Exp Biol*. 1987;1(5):365–74.
  40. Akaike H. New look at the statistical model identification. *IEEE Trans Autom Control*. 1974;AC-19(6):716–23.
  41. Burnham KP, Anderson DR. Model Selection and Multimodel Inference: A Practical Information-Theoretic Approach. Springer Science & Business Media; 2002. 528 p.
  42. Ross T, McMeekin TA. Predictive microbiology. *Int J Food Microbiol*. 1994;23(3–4):241–64.
  43. Gibson AM, Bratchell N, Roberts TA. The effect of sodium chloride and temperature on the rate and extent of growth of *Clostridium botulinum* type A in pasteurized pork slurry. *J Appl Bacteriol*. 1987;62(6):479–90.
  44. Johnsen AR, Binning PJ, Aamand J, Badawi N, Rosenbom AE. The Gompertz function can coherently describe microbial mineralization of growth-sustaining pesticides. *Environ Sci Technol*. 2013;47(15):8508–14.
  45. McKellar RC, Knight K. A combined discrete-continuous model describing the lag phase of *Listeria monocytogenes*. *Int J Food Microbiol*. 2000;54(3):171–80.
  46. Membré J-M, Ross T, McMeekin T. Behaviour of *Listeria monocytogenes* under combined chilling processes. *Lett Appl Microbiol*. 1999;28(3):216–20.
  47. Whiting RC. Modeling bacterial survival in unfavorable environments. *J Ind Microbiol*. 1993;12(3–5):240–6.
  48. Bolker BM. Ecological Models and Data in R. Princeton, N.J: Princeton University Press; 2008. 408 p.